Published in final edited form as:
Biomaterials. 2013 February ; 34(5): 1529–1536. doi:10.1016/j.biomaterials.2012.10.070.

Templated Agarose Scaffolds for the Support of Motor Axon Regeneration Into Sites of Complete Spinal Cord Transection

Mingyong Gao[1], **Paul Lu**[1,2], **Bridget Bednark**[3], **Dan Lynam**[3], **James M Conner**[1], **Jeff Sakamoto**[3], and **Mark Tuszynski**[1,2,*]

[1] Department of Neurosciences, University of California-San Diego, La Jolla, CA 92093, USA

[2] Veterans Affairs Medical Center, San Diego, CA 92161, USA

[3] Department of Chemical Engineering and Materials Science, Michigan State University, East Lansing, MI 48824, USA

Abstract

Bioengineered scaffolds have the potential to support and guide injured axons after spinal cord injury, contributing to neural repair. In previous studies we have reported that templated agarose scaffolds can be fabricated into precise linear arrays and implanted into the partially injured spinal cord, organizing growth and enhancing the distance over which local spinal cord axons and ascending sensory axons extend into a lesion site. However, most human injuries are severe, sparing only thin rims of spinal cord tissue in the margins of a lesion site. Accordingly, in the present study we examined whether template agarose scaffolds seeded with bone marrow stromal cells secreting Brain-Derived Neurotrophic Factor (BDNF) would support regeneration into severe, complete spinal cord transection sites. Moreover, we tested responses of motor axon populations originating from the brainstem. We find that templated agarose scaffolds support motor axon regeneration into a severe spinal cord injury model and organize axons into fascicles of highly linear configuration. BDNF significantly enhances axonal growth. Collectively, these findings support the feasibility of scaffold implantation for enhancing central regeneration after even severe central nervous system injury.

INTRODUCTION

Axons of the central nervous system fail to spontaneously regenerate after spinal cord injury, frequently resulting in permanent deficits of motor, sensory or autonomic function. Several experimental strategies can enhance the growth of central axons, including growth factors [1, 2], stimulation of the intrinsic neuronal growth state [3, 4], neutralization of inhibitors to axon growth in the injured central nervous system environment [5, 6], and placement of a matrix to support axon growth in the lesion site [7]. Most matrices placed into spinal cord lesion sites to support axonal growth have consisted of cells, including bone marrow stromal cells, Schwann cells, fibroblasts, astrocytes or olfactory ensheathing cells [8–13]. While these cell types support axonal attachment and extension, axons fail to retain their native organization into fascicles of related function, resulting in axonal growth into the lesion that is disorganized and circuitous in pattern [14].

*Correspondence: mtuszynski@ucsd.edu Phone 858 534 8857 FAX: 858 534 5220.

Bioengineered scaffolds offer the potential to organize axonal growth to mimic the natural organization and orientation of axons as they extend through a lesion site. To accomplish this goal, scaffolds should hypothetically contain several individual compartments that bundle axons of related function, and should maintain a strictly linear configuration over distances of several millimeters in rodent models of spinal cord injury (and several centimeters for potential human translation; Fig. 1) to prevent mistargeting from one fascicle of specific function to another fascicle of different function. In addition, the scaffold should consist of a material that elicits a minimal host inflammatory response, and should be capable of releasing growth-promoting substances such as growth factors [15, 16]. Finally, the scaffold should exhibit elastic moduli resembling the normal spinal cord to minimize mechanical parenchymal damage at points of contact between the scaffold and host.

For the past several years we have been exploring the properties of bioengineered agarose scaffolds in models of spinal cord injury. Through an extrusion/fusion process, this material can be fabricated into strictly linear channels over lengths of several centimeters. When seeded with autologous bone marrow stromal cells secreting growth factors, scaffolds support host axonal growth in strictly linear arrays over the full length of a lesion site and in relatively high density [14, 17]. Growth of axons arising from intrinsic neuronal pools of the spinal cord, and of sensory axons projecting from the periphery, has been observed in partial spinal cord lesion models [14, 17]. These studies have provided important proof-of-concept indicating that bioengineered scaffolds, under ideal conditions, can support, organize and linearize axon growth through a lesion site.

The present study assessed whether bioengineered scaffolds have the potential to support and guide axonal growth in a more clinically relevant model of severe spinal cord injury. Adult rats underwent a severe lesion consisting of complete spinal cord transection, with placement of templated agarose scaffolds into the lesion site. Some implants were seeded with syngenic bone marrow stromal cells that secrete the growth factor Brain-Derived Neurotrophic Factor (BDNF). Moreover, we studied responses of axons originating in the brain that control specific components of motor function. We now report in a severe, complete transection model of spinal cord injury that templated agarose scaffolds support and guide motor axonal regeneration over the full length of the lesion.

MATERIALS AND METHODS

Fabrication of Templated Agarose Scaffolds

To generate agarose scaffolds, multi-component fiber bundle (MCFB) templates were fabricated from 200μm diameter polystyrene fibers (Paradigm Optics, Vancouver, WA) arranged in a hexagonal close-packed array separated by a continuous matrix of poly (methyl methacrylate) (PMMA), as previously described [17]. Polystyrene fibers of 166μm diameter were arranged with 66μm interval spacing in a honeycomb array to generate final scaffolds with wall sizes of 66μm and channel diameters of 166μm (Fig. 1). Bundles were simultaneously extruded and fused such that polystyrene fibers were oriented parallel to the longitudinal axis of the bundles. The multi-component fiber bundle templates were trimmed to a length of 2mm and a cross-sectional width and depth of 1.5mm (Fig. 1). Polystyrene end caps 1.5 mm in length were bonded to fiber bundle terminals using cyclohexane to anchor polystyrene fibers and form an external, rigid multi-component fiber bundle template. Six such multi-component fiber bundle units were then aligned in-series with 2 polystyrene side caps agglutinating into a linear template array. The poly-methylmethacrylate matrix was then selectively removed by immersion in 99.7% propylene carbonate (Sigma-Aldrich) three times, followed by 95% ethanol rinse and distilled water rinse.

Ultrapure agarose (30 mg/ml, Sigma-Aldrich) was dissolved in distilled water at 100°C and then cooled to 65°C. Multi-component fiber bundle templates were submerged into the agarose solution and centrifuged (300rpm for 30sec) to permeate agarose through the packed polystyrene fiber array. The agarose cast was then allowed to gel at room temperature, trimmed, and immersed in 99% tetrahydrofuran (Sigma-Aldrich) at room temperature for 24hr. This was repeated twice to remove the polystyrene mold, resulting in individual free-floating agarose scaffolds. The scaffolds were collected and washed sequentially in acetone, 95% ethanol, and three cycles of sterile water. They were stored in sterile water at room temperature until use. The final scaffolds for implantation had channels of 166μm diameter separated in a honeycomb arrangement consisting of 66μm walls.

Preparation of Bone Marrow Stromal Cells and BDNF Expressing Vectors

To prepare bone marrow stromal cells for filling of scaffolds in some groups of animals, Fischer 344 adult female rats were anesthetized with a cocktail (2 ml/kg) of ketamine (25 mg/ml), xylazine (1.3mg/ml), and acepromazine (0.25 mg/ml). Rats were rapidly decapitated, and tibias/femurs were removed. The end caps of each bone were removed, and 5ml of α-MEM (Invitrogen, Carlsbad, CA) was injected into the bone medulla to extrude marrow. Cells were cultured in α-MEM supplemented with 20% fetal bovine serum and antibiotics. Cells were passaged twice and non-adherent cells were removed during media changes, as previously described [18].

Previously we generated stable PA317 retrovirus producer cell lines containing Moloney-leukemia virus (MLV)-based retroviral vectors coding for full length human BDNF[18]. Conditioned media from these producer cell lines was added to marrow stromal cell cultures and cells that successfully incorporated the transgene were selected in G418 medium (100mg/ml) for 10–14d. After selection was complete, cells were allowed to grow to confluence, and 24 h supernatants were collected for ELISA of BDNF protein levels (BDNF Emax ImmunoAssay System; Promega, Madison, WI). These syngenic transduced marrow stromal cells produced between 135 – 160ng BDNF/10^6cells/day, an amount exceeding physiological levels by approximately 1000-fold. Cells were frozen until use. Control cells expressed the reporter gene Green Fluorescent Protein (GFP).

Surgical Procedures

A total of 57 adult female Fischer 344 rats (150–200g) were subjects of this study. NIH guidelines for laboratory animal care and safety were followed. Animals were randomly divided into one of three experimental groups, as follows: **Group 1** (N=26 animals) underwent complete T3 transection lesions, and implants into the lesion site of 2mm-long templated agarose scaffolds that were loaded with syngenic marrow stromal cells expressing BDNF; **Group 2** (N=25 animals) underwent complete T3 transection lesions, and implants into the lesion site of scaffolds that were loaded with syngenic marrow stromal cells expressing the reporter gene Green Fluorescent Protein (GFP); **Group 3** (N=6 animals) underwent complete T3 transection lesions, and implants into the lesion site of 2mm-long templated agarose scaffolds that did not contain cells. Animals were sacrificed four weeks after lesions and scaffold implantation.

For surgical procedures, animals were anesthetized with a combination (2 ml/kg) of ketamine (25 mg/ml), xylazine (1.3 g/ml), and acepromazine (0.25mg/ml). A T2–T4 laminectomy was performed and dura was opened, and the spinal cord was transected at the T3 spinal segment using a combination of microscissors and microaspiration. A block of spinal cord was excised under microscopic guidance to produce a 1.8mm-long complete transection cavity. The lesion cavity was carefully inspected to ensure lesion completeness ventrally and laterally. Scaffolds were then loaded with cells in Groups 1 and 2 (marrow

stromal cells at a density of 5×10^5cells/μl), and scaffolds in all groups were then implanted into the lesion cavity using microforceps. Care was taken to ensure snug apposition of the rostral and caudal interfaces of scaffolds with the host spinal cord, and to ensure proper rostral-caudal alignment of the scaffold with the longitudinal axis of the spinal cord. The dura was closed with 9–0 microsurgical suture (Ethicon), and a surgical steel wire was used to stabilize the T2–T6 spinous processes to prevent movement of the surgical site. After surgery, rats were housed separately with access to food and water ad libitum on a 12:12 h light/dark cycle. Antibiotics were administered twice daily for two weeks and bladders were manually emptied by gentle massage until reflex bladder emptying recovered in approximately 10 days.

In all groups, the reticulospinal tract (RST) was anterogradely labeled by injecting 0.5μl of a 10% biotinylated dextran amine (BDA, MW10,000, invitrogen, CA) solution into the gigantocellular pontine reticular nucleus using a glass micropipette in four sites per side. Site 1: AP −11mm, lateral 0.8 mm, depth 7.3mm. Site 2: AP −12.5 mm, lateral 0.8 mm, depth 7.3mm. Site 3: AP −11mm, lateral 0.8 mm, depth 8.2 mm. Site 4: AP −12.5mm, lateral 0.8 mm, and depth 8.2mm (Jin et al., 2002). Injections were made using a PicoSpritzer pneumatic injection system (General Valve, Inc.), three weeks before animal sacrifice. For transganglionic labeling of long distance ascending sensory projections. Animals used for histological analysis received injections of cholera toxin B (CTB) (1%, 2 μl per side; List Biologic, Campbell, CA) into bilateral sciatic nerves 3 d before sacrifice to label the ascending sensory projections.

Tissue Preparation and Labeling

Four weeks after scaffold implantation, animals were transcardially perfused with 4% paraformaldehyde in 0.1 M phosphate buffer (pH 7.4) at 4°C. Spinal cord segments 2cm in length centered about the lesion site were collected and post-fixed in 4% PFA overnight at 4°C, then imm ersed into 30% sucrose (w/v, Sigma) in 0.1 M phosphate buffer at 4°C for a n additional 48h prior to cryosectioning. Serial parasagittal sections were collected on a cryostat set at 30μm thickness. 1-in-7 sections (spaced 210μm apart) were mounted on gelatin-coated slides for Nissl stain for general cellular labeling. The remaining sections were serially collected for immunocytochemistry. To visualize BDA labeling of reticulospinal tract (RST) or raphespinal tract (5-HT) axons, sections were blocked for endogenous peroxidase activity with 0.6% hydrogen peroxide in 100% methanol for 15 min at room temperature, then rinsed with Tris-buffered saline (TBS). For BDA labeling, sections were incubated overnight with avidin-biotinylated peroxidase complex (1:100, Vector Elite Kid) in TBS containing 0.25% Triton X-100 at 4°C. Diaminobenzidine (0.05%) with nickel chloride (0.04%) was used as a chromagen, with reactions sustained for 1–6 min at room temperature. For 5-HT labeling, sections were blocked with 5% goat serum in TBS containing 0.25% Triton X-100 for 1h. Sections were incubated overnight with Rabbit-anti-serotonin (5-HT; monoclonal antibody from Chemicon at 1:1500), followed by incubation with HRP-conjugated Goat anti-Rabbit IgG (1:10 dilution) for 2h at room temperature. Peroxidase was visualized with diaminobenzidine enhanced by nickel chloride. For visualization of CTB labeling, sections were incubated at 4°C for 48h in goat anti-CTB primary antibody (1:10,000); followed by biotinylated horse anti-goat IgG (1:200; Vector Laboratories, Burlingame, CA). Avidin-biotinylated peroxidase complex (1:150; Vector Elite kit; Vector Laboratories) was then added at room temperature and labeling was visualized by nickel chloride intensification. The sections were then mounted on gelatin-coated slides, dehydrated, and coverslipped with Pro-Texx mounting medium (Baxter Diagnostics, Deerfield, IL). For immunofluorescent labeling, sections were first blocked with 5% donkey serum, then every seventh section was incubated with the following primary antibody combinations: Alexa 594-conjugated streptavidin for reticulospinal BDA

labeling (1:100, invitrogen, CA); mouse-anti-NF200 (1:1000, Chemicon, Temecula, CA) to label larger diameter axons; or goat anti-ChAT (1:100, Chemicon, Temecula, CA) to label spinal cord motor axons or sympathetic axons. After incubation with primary antibody overnight at 4°C followed by washes in TBS-Triton, sections were incubated with fluorescein-conjugated secondary antibody combinations: donkey-anti-rabbit Alexa 488, donkey-anti-mouse 594, or donkey-anti-goat 594 (1:200, invitrogen, CA) for 2.5h. Sections were washed, mounted on uncoated slides and coverslipped with Fluoromount G (Southern Biotechnology Associates, Inc.).

Quantification of Axons Within Scaffolds

Axonal number within scaffolds was quantified using Image J (version 1.43; NIH, Bethesda, MD), as previously described [18]. Briefly, quantification was performed at intervals within channels located 0–500, 750–1250, and 1500–2000μm caudal to the rostral host-implant interface. Within each interval, three randomly selected channels were chosen from a series of 3-of-7 sections from each subject. Images were converted to black and white and the number of pixels occupied by immunolabeled axons within a fixed box size of 640×480 pixels at 200× magnification was measured in sections immunolabeled for BDA, 5-HT, NF and ChAT in subjects from each group. Thresholding values on images were set to detect immunolabeled axons, and nonspecific background labeling and artifactual spots were edited from images. Total labeled pixels were divided by the sampling box size (640×480 pixels) to obtain mean axon density; results were expressed as mean pixels per channel. Results are expressed as mean ± SEM.

Statistical Analysis

Multiple group comparisons were performed by Kruskall Wallis test, with Dunn post-hoc test and Bonferroni correction for multiple comparisons. Axonal quantification was performed by the first author of the study, who states that he was blinded to group identity.

RESULTS

Scaffold Integration into Lesion Site

Scaffolds exhibited excellent integration into the complete transection site when examined four weeks after implantation (Fig. 1). Previously we reported the formation of reactive cell layers at host/scaffold interfaces placed in smaller, partial spinal cord lesion sites [14, 17]. In this severe, complete transection model, formation of thin reactive cell layers were detected on Nissl stains at host/scaffold interfaces, but were not qualitatively thicker or more severe in extent than previous implants into partial lesion models (compare Fig. 1A–C to Fig. 1E in [14]). The rostral-to-caudal length of the reactive cell layer depended on the precision of scaffold placement into the lesion site: larger reactive cell layers formed when more disruption of host parenchyma occurred during implantation, particularly with scaffold re-positioning to optimize “fit”. Scaffold integration into the lesion site, and size of the reactive cell layer, did not qualitatively differ among groups receiving empty scaffolds, scaffolds with bone marrow stromal cells, or scaffolds with bone marrow stromal cells secreting BDNF (Fig. 1C–F). Consistent with previous observations [14, 17], scaffolds did not biodegrade over the 4-week period of this experiment.

Brainstem Motor and Local Axons Regenerate into Scaffolds, Adopting Precisely Linear Directions of Growth

Brainstem reticular motor axons activate spinal systems primarily involved in reflex motor activity, including posture and gait [18–20]. Previous reports indicate that these axons respond to BDNF, exhibiting increased growth into a non-organized cell suspension graft

placed in a spinal cord lesion cavity[21]. In the present experiment, brainstem reticular motor axons regenerated into scaffolds containing cell implants placed in the lesion site (BDNF-secreting and GFP-expressing; Fig. 2). Axonal growth was highly linear in orientation (Fig. 2). A significantly greater number of axons penetrated scaffolds pre-filled at the time of implantation with bone marrow stromal cells as a cell substrate (Figs. 2, 4); moreover, secretion of BDNF by implanted marrow stromal cells further amplified the number of motor axons penetrating the lesion site (Figs. 2,3). Axons regenerated the full length of the lesion cavity only in the BDNF-secreting group (Figs. 2, 4). In no case were motor axons observed to regenerate beyond the scaffold in the lesion site, however.

Brainstem serotonergic axons also modulate spinal cord motor function [22–25], and respond to BDNF [21]. Similar to findings with brainstem motor axons, serotonergic axons penetrated the channels of scaffolds placed in the lesion site, extended the full length of the lesion cavity, and grew in greater numbers (but the same distance) in the presence of cell grafts and BDNF secretion (Figs 3, 4). Similar growth of ChAT-labeled axons, possibly arising from local motor neurons, cholinergic partition cells, or sympathetic neurons of the intermediolateral cell column, was observed.

Axonal systems in the spinal cord project bi-directionally: generally, motor systems descend the spinal cord and sensory systems ascend, separated into distinct functional fascicles. We labeled ascending sensory axons with injections of the transganglionic tracer cholera toxin B subunit (CTB) into the sciatic nerve, 72 hours prior to perfusion. Sensory axons also regenerated into scaffolds, with the highest numbers of axons present in scaffolds containing BDNF-secreting marrow stromal cells (Figs. 3,4).

DISCUSSION

To advance in clinical relevance, it is important to examine the ability of bioengineered scaffolds to support, orient and guide axonal growth in clinically relevant models of spinal cord injury. Advancing this objective, the present results indicate that in the most severe model of spinal cord injury, complete transection, bioengineered scaffolds are retained in sites of injury over long time periods and are capable of guiding axons. Consistent with previous reports in partial lesion models that examined non-motor axonal populations [14], we find that these scaffolds support highly linear axonal extension of several motor axon populations over the full distance of the lesion site. Secretion of the growth factor BDNF significantly increases the number of axons regenerating into scaffold channels.

Additional development work in moving toward clinical application is needed. An important development objective is the elicitation of axonal growth not only into, but beyond, the channels of the scaffold placed in the lesion site and into host spinal cord. Reactive cellular interfaces between host and scaffold may limit axonal egress from the lesion [14]. The provision of growth factor gradients beyond the lesion may stimulate axonal egress in future scaffold experiments, as observed in experiments using non-organized cell grafts to the lesion site [1], or degradation of inhibitory barriers in the spinal cord [26–28]. Alternatively, or in combination, stimulation of the intrinsic growth state of the injured axon may propel axonal regeneration beyond the lesion [29–33].

Another important step in the translation of bioengineered scaffold technology to clinical relevance will be the testing of scaffolds in severe contusion models of spinal cord injury. The pathological mechanism of most human injuries is contusion [34, 35], which results in a cystic lesion cavity that is often cylindrically shaped with tapering edges at rostral and caudal interfaces (Fig. 5). This type of lesion is distinct in morphology from transection injury models, which create a lesion cavity with cleaner “edges” (Figs. 1–4). While self-

assembling matrices are hypothetically advantageous for application to cylindrical, tapering lesion morphologies, current self-assembly technology does not support the formation of precise, high-fidelity linear arrays over long-distances, and linear guidance channels will likely be required to appropriately guide regenerating axons toward appropriate target regions in the injured spinal cord. Placement of contusion injuries at thoracic levels in animal models would allow subsequent re-shaping of the lesion cavity at rostral and caudal interfaces to create perpendicular edges to accommodate the implantation of scaffolds, since little additional clinical deficit would occur upon re-shaping a thoracic level injury (Fig. 5). Alternatively, cell suspensions could be placed in the tapering components of contusion injuries together with scaffolds in the major portion of the lesion (Fig. 5); this approach might reduce but not eliminate axon guidance over short distances, while retaining linear axon guidance over the majority distance of the lesion site in scaffold channels.

Growth factor gene delivery significantly enhanced the number of motor axons regenerating into scaffold channels in this experiment, consistent with previous findings using disorganized cell suspension grafts [9, 21] and scaffolds [14, 17]. Clinical application might be simplified if growth factors were slowly released from scaffolds, rather than delivered by gene transfer. Biomaterials can provide protracted release of loaded proteins over time [15, 16, 36], a technology that should be incorporated into the present design.

CONCLUSION

We report that bioengineered scaffolds can support, orient and guide the regeneration of motor axons in a severe model of spinal cord injury, complete transection. Future work will focus on promoting axonal regeneration beyond the lesion, and reduction to yet more clinically relevant models, including severe contusion lesions.

Acknowledgments

This work was supported by the NIH/NIBIB (R01EB014986), the Veterans Administration, The Craig H. Neilsen Foundation, and the Bernard and Anne Spitzer Charitable Trust.

REFERENCES

[1]. Alto LT, Havton LA, Conner JM, Hollis Ii ER, Blesch A, Tuszynski MH. Chemotropic guidance facilitates axonal regeneration and synapse formation after spinal cord injury. Nature Neurosci. 2009; 12:1106–13. [PubMed: 19648914]

[2]. Giger RJ, Hollis ER 2nd, Tuszynski MH. Guidance molecules in axon regeneration. Cold Spring Harbor Perspec Biol. 2010; 2:a001867.

[3]. Pearse DD, Pereira FC, Marcillo AE, Bates ML, Berrocal YA, Filbin MT, et al. cAMP and Schwann cells promote axonal growth and functional recovery after spinal cord injury. Nature Med. 2004; 10:610–6. [PubMed: 15156204]

[4]. Neumann S, Bradke F, Tessier-Lavigne M, Basbaum AI. Regeneration of sensory axons within the injured spinal cord induced by intraganglionic cAMP elevation. Neuron. 2002; 34:885–93. [PubMed: 12086637]

[5]. Filbin MT. Myelin-associated inhibitors of axonal regeneration in the adult mammalian CNS. Nat Rvw Neurosci. 2003; 4:703–13.

[6]. Fitch, MT.; Silver, J. Glial Cells, Inflammation and CNS Trauma. In: Kordower, JA.; Tuszynski, MH., editors. CNS Regeneration: Basic Science and Clinical Advances. 2nd ed.. Elsvier; San Diego: 2008.

[7]. Blesch A, Tuszynski MH. Spinal cord injury: plasticity, regeneration and the challenge of translational drug development. TINS. 2009; 32:41–7. [PubMed: 18977039]

[8]. Kuhlengel KR, Bunge MB, Bunge RP, Burton H. Implantation of cultured sensory neurons and Schwann cells into lesioned spinal cord. II. Implant characteristics and examination of corticospinal tract growth. J Comp Neurol. 1990; 293:74–91. [PubMed: 1690226]

[9]. Tuszynski MH, Peterson DA, Ray J, Baird A, Nakahara Y, Gage FH. Fibroblasts genetically modified to produce nerve growth factor induce robust neuritic ingrowth after grafting to the spinal cord. Exp Neurol. 1994; 126:1–14. [PubMed: 8157119]

[10]. Biernaskie J, Sparling JS, Liu J, Shannon CP, Plemel JR, Xie Y, et al. Skin-derived precursors generate myelinating Schwann cells that promote remyelination and functional recovery after contusion spinal cord injury. J Neurosci. 2007; 27:9545–59. [PubMed: 17804616]

[11]. Richter MW, Roskams AJ. Olfactory ensheathing cell transplantation following spinal cord injury: hype or hope? Exp Neurol. 2008; 209:353–67. [PubMed: 17643431]

[12]. Grill R, Murai K, Blesch A, Gage FH, Tuszynski MH. Cellular delivery of neurotrophin-3 promotes corticospinal axonal growth and partial functional recovery after spinal cord injury. J Neurosci. 1997; 17:5560–72. [PubMed: 9204937]

[13]. Nomura H, Kim H, Mothe A, Zahir T, Kulbatski I, Morshead CM, et al. Endogenous radial glial cells support regenerating axons after spinal cord transection. Neuroreport. 2010; 21:871–6. [PubMed: 20671580]

[14]. Gros T, Sakamoto JS, Blesch A, Havton LA, Tuszynski MH. Regeneration of long-tract axons through sites of spinal cord injury using templated agarose scaffolds. Biomaterials. 2010; 31:6719–29. [PubMed: 20619785]

[15]. Wylie RG, Ahsan S, Aizawa Y, Maxwell KL, Morshead CM, Shoichet MS. Spatially controlled simultaneous patterning of multiple growth factors in three-dimensional hydrogels. Nature Mater. 2011; 10:799–806. [PubMed: 21874004]

[16]. Willerth SM, Johnson PJ, Maxwell DJ, Parsons SR, Doukas ME, Sakiyama-Elbert SE. Rationally designed peptides for controlled release of nerve growth factor from fibrin matrices. J Biomed Mater Res Part A. 2007; 80:13–23.

[17]. Stokols S, Sakamoto J, Breckon C, Holt T, Weiss J, Tuszynski MH. Templated agarose scaffolds support linear axonal regeneration. Tissue Eng. 2006; 12:2777–87. [PubMed: 17518647]

[18]. Lawrence DG, Kuypers HGJM. The functional organization of the motor system in the monkey. II. The effects of lesions of the descending brain-stem pathways. Brain. 1968; 91:15–36. [PubMed: 4966860]

[19]. Baker SN. The primate reticulospinal tract, hand function and functional recovery. J Physiol. 2011; 589:5603–12. [PubMed: 21878519]

[20]. Szokol K, Glover JC, Perreault MC. Differential origin of reticulospinal drive to motoneurons innervating trunk and hindlimb muscles in the mouse revealed by optical recording. J Physiol. 2008; 586:5259–76. [PubMed: 18772205]

[21]. Lu P, Jones LL, Tuszynski MH. BDNF-expressing marrow stromal cells support extensive axonal growth at sites of spinal cord injury. Exp Neurol. 2005; 191:344–60. [PubMed: 15649491]

[22]. Jacobs BL, Fornal CA. Serotonin and motor activity. Curr Opin Neurobiol. 1997; 7:820–5. [PubMed: 9464975]

[23]. Alvarez FJ, Pearson JC, Harrington D, Dewey D, Torbeck L, Fyffe RE. Distribution of 5-hydroxytryptamine-immunoreactive boutons on alpha-motoneurons in the lumbar spinal cord of adult cats. J Comp Neurol. 1998; 393:69–83. [PubMed: 9520102]

[24]. Jordan LM, Liu J, Hedlund PB, Akay T, Pearson KG. Descending command systems for the initiation of locomotion in mammals. Brain Res Rev. 2008; 57:183–91. [PubMed: 17928060]

[25]. Hornung JP. The human raphe nuclei and the serotonergic system. J Chem Neuroanat. 2003; 26:331–43. [PubMed: 14729135]

[26]. Bradbury EJ, Moon LD, Popat RJ, King VR, Bennett GS, Patel PN, et al. Chondroitinase ABC promotes functional recovery after spinal cord injury. Nature. 2002; 416:636–40. [PubMed: 11948352]

[27]. Garcia-Alias G, Barkhuysen S, Buckle M, Fawcett JW. Chondroitinase ABC treatment opens a window of opportunity for task-specific rehabilitation. Nat Neurosci. 2009; 12:1145–51. [PubMed: 19668200]

[28]. Tom VJ, Sandrow-Feinberg HR, Miller K, Santi L, Connors T, Lemay MA, et al. Combining peripheral nerve grafts and chondroitinase promotes functional axonal regeneration in the chronically injured spinal cord. J Neurosci. 2009; 29:14881–90. [PubMed: 19940184]

[29]. Lu P, Yang H, Jones LL, Filbin MT, Tuszynski MH. Combinatorial therapy with neurotrophins and cAMP promotes axonal regeneration beyond sites of spinal cord injury. J Neurosci. 2004; 24:6402–9. [PubMed: 15254096]

[30]. Kadoya K, Tsukada S, Lu P, Coppola G, Geschwind D, Filbin MT, et al. Combined intrinsic and extrinsic neuronal mechanisms facilitate bridging axonal regeneration one year after spinal cord injury. Neuron. 2009; 64:165–72. [PubMed: 19874785]

[31]. Lu P BA, Graham L, Wang W, Samara R, Banos K, Haringer V, Havton L, Weishaup N, Bennett D, Fouad K, Tuszynski MH. Motor axonal regeneration after partial and complete spinal cord transection. J Neurosci. 2012; 32:8208–18. [PubMed: 22699902]

[32]. Alilain WJ, Horn KP, Hu H, Dick TE, Silver J. Functional regeneration of respiratory pathways after spinal cord injury. Nature. 2011; 475:196–200. [PubMed: 21753849]

[33]. Sun F, Park KK, Belin S, Wang D, Lu T, Chen G, et al. Sustained axon regeneration induced by co-deletion of PTEN and SOCS3. Nature. 2011; 480:372–5. [PubMed: 22056987]

[34]. Young W. Spinal cord contusion models. Prog Brain Res. 2002; 137:231–55. [PubMed: 12440371]

[35]. Steeves JD, Lammertse D, Curt A, Fawcett JW, Tuszynski MH, Ditunno JF, et al. Guidelines for the conduct of clinical trials for spinal cord injury (SCI) as developed by the ICCP panel: clinical trial outcome measures. Spinal Cord. 2007; 45:206–21. [PubMed: 17179972]

[36]. Mehrotra S, Lynam D, Maloney R, Pawelec KM, Tuszynski MH, Lee I, et al. Time controlled protein release from layer-by-layer Assembled multilayer functionalized agarose hydrogels. Adv Func Mater. 2010; 20:247–58.

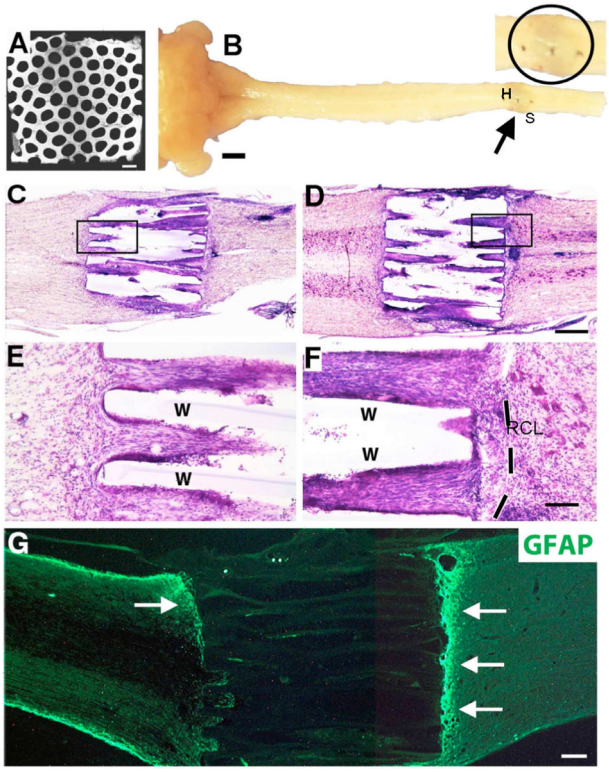

Figure 1. Scaffold Implantation into T3 Complete Transection Site

(**A**) Cross section of scaffold revealing macroscopic architecture. Channels are 200μm in diameter and walls are 66μm, in honeycomb arrangement. Scanning EM. (**B**) Gross appearance of scaffold implanted into complete thoracic transection site (arrow), one month after injury. Dorsal aspect of spinal cord. Arrow indicates scaffold in complete T3 transection site; this region is shown at higher magnification in the adjoining image, with the actual scaffold implant site circled. The three dark spots in the image are dural sutures. (**C–F**) Scaffold integration into complete transection site on Nissl stain with Horizontal sections. (**C,E**) Lesion site containing scaffold pre-loaded with GFP-expressing bone marrow stromal cells. Higher magnification in **E** shows excellent scaffold integration with host spinal cord and numerous cells in channels. Walls of scaffolds are indicated by “W”. (**D, F**) Scaffold pre-loaded with BDNF-expressing bone marrow stromal cells. Once again, scaffold exhibits excellent integration with host and minimal reactive cell layer, visible more clearly in **F** (dashed line). (**G**) GFAP labeling shows upregulation of glial reactivity (arrows) at interfaces with lesion site. Other regions of scaffold interface with host are free of GFAP upregulation, e.g., in lower left section of scaffold in G. Scale bar: A, 500μm; B, 2mm; C,D, 400μm; E,F, 100μm; G, 225μm.

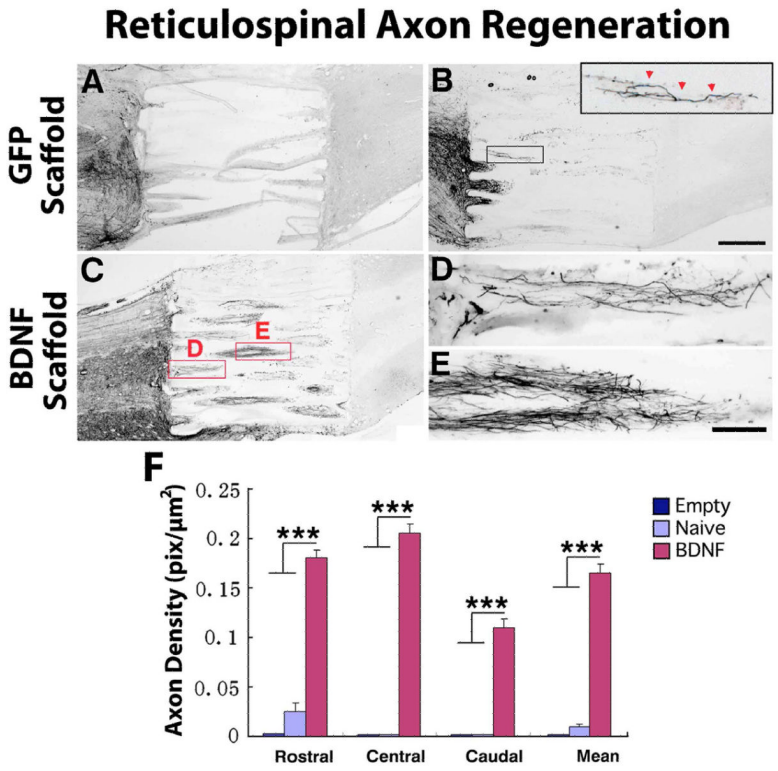

Figure 2. Regeneration of BDA-labeled Reticulospinal Motor Axons into Templated Agarose Scaffolds in Complete Transection Sites

(**A**) Empty scaffolds contained very few regenerating reticulospinal axons and these extended for only short distances in the lesion site. In all panels rostral is to the left. Such scaffolds, nearly devoid of regenerating axons, tended to distort on histological processing. (**B**) Scaffolds filled with a cellular matrix of bone marrow stromal cells expressing the reporter gene GFP, but not expressing a growth factor, exhibited modest axonal penetration of scaffolds but these failed to extend to distal aspects of the lesion site (inset). (**C**) Scaffolds filled with BDNF-secreting marrow stromal cells exhibited significant increases in the total number of axons entering scaffolds and in total axons reaching the distal aspect of the lesion site, quantified in panel F. Higher magnification views of (**D**) axonal entry into scaffold channels, and (**E**) midway through lesion, are shown at higher magnification. Axons invariably extended in linear trajectories. However, axons did not regenerate into host spinal cord tissue beyond the lesion site. (**F**) Quantification of axonal density in scaffolds at short (0–500μm), middle (750–1250μm) and caudal (1500–2000μm) aspects of channels. Kruskall Wallis test, χ^2 $p<0.01$; Dunn post-hoc with Bonferroni correction ***$p< 0.001$. Asterisks indicate comparisons of BDNF group to both Empty and Naïve groups. Error bars indicate SEM. Scale bar: A–C 500μm; D, E 100μm.

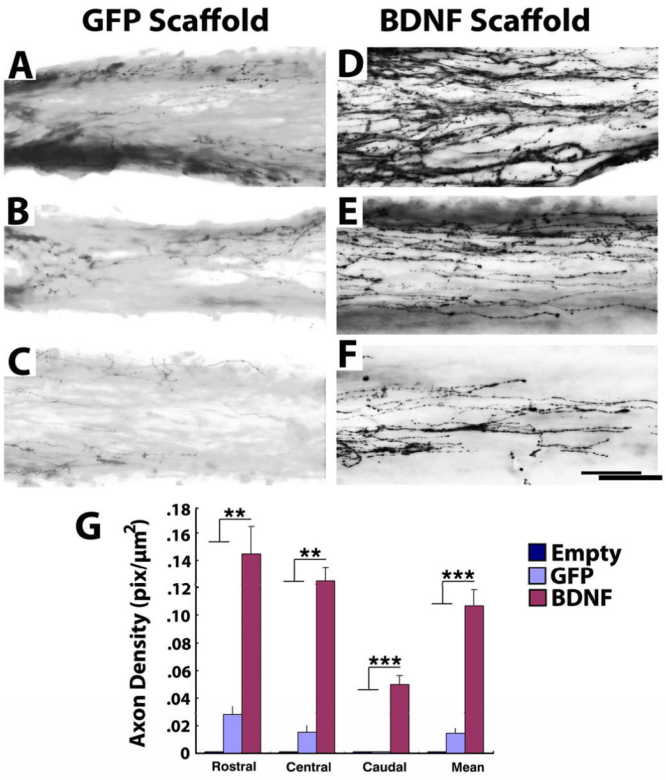

Figure 3. Regeneration of Serotonergic Axons into Templated Agarose Scaffolds in Complete Transection Sites

(**A–C**) Modest numbers of serotonergic axons labeled for 5HT penetrate scaffolds filled with GFP-expressing marrow stromal cells. **A**, entry into scaffold; **B**, mid-point of scaffold; **C**, caudal aspect of channel. (**D**) Significantly greater numbers of serotonergic axons penetrate scaffolds filled with BDNF-secreting marrow stromal cells, quantified in **G**. **D**, axonal entry into channel; **B**, mid-point of scaffold; **C**, caudal aspect of channel. Axons extended in linear trajectories. (**G**) Kruskall Wallis test, χ^2 $p<0.01$; Dunn post-hoc with Bonferroni correction $^{**}p<0.01$, $^{***}p< 0.001$. Asterisks indicate comparisons of BDNF group to both Empty and Naïve groups. Scale bar: **A–C**, 500μm; **E–I**, 50μm.

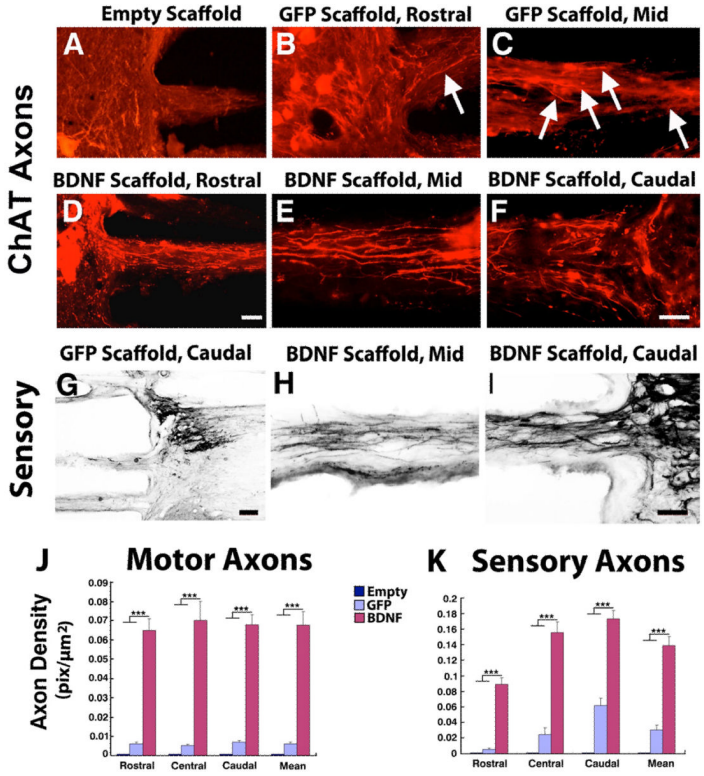

Fig. 4. Regeneration of Local Motor and Ascending Sensory Axons into Scaffolds

(**A**) Choline acetyltransferase (ChAT)-expressing local neurons did not extend axons into empty scaffolds. (**B**) Scaffolds containing GFP-expressing cells contained modest axonal numbers, that (**C**) extended to the mid-portion of the lesion site. (**D–F**) Filling of scaffolds with BDNF-secreting marrow stromal cells resulted in an increased number of axons that extended over the full extent of the complete lesion site, quantified in **J.** Substantially greater numbers of axons are visible compared to panels A–C. Axons extended in linear configurations. (**G**) Similarly, sensory axons arising from the sciatic nerve extended in modest numbers into scaffolds loaded with GFP-expressing cells, and (**H, I**) regenerated in greater numbers and over greater distances in scaffolds loaded with BDNF-secreting cells, as quantified in **K.** (**J, K**) Kruskall Wallis test, χ^2 $p<0.01$; Dunn post-hoc with Bonferroni correction, ***$p< 0.001$. Asterisks indicate comparisons of BDNF group to both Empty and Naïve groups. Scale bars A–F, H,I, 100μm; G, 250μm.

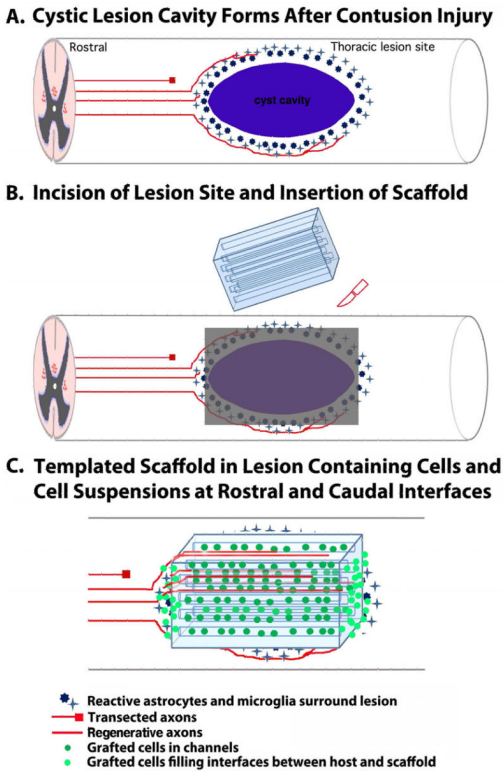

Figure 5. Model for Scaffold Implantation in Clinically Relevant Contusive Spinal Cord Injury

(**A**) Human spinal cord injuries result in oval cystic lesion cavities that interrupt projecting axons (red) and cause demyelination. Scaffold implantation into this type of lesion would involve (**B**) placement of a dorsal linear incision in the spinal cord to provide a window for scaffold implantation, and (**C**) insertion of the scaffold. Because the original lesion is oval shaped, scaffolds would either need to be fabricated in a manner to match the shape of the lesion, or placed in a manner to occupy less than the full volume of the lesion site (shown in this example). The interfaces would then be filled with a cell matrix.